

# Scintillation Properties of Eu-doped SrF<sub>2</sub> Transparent Ceramics

Takumi Kato,\* Daisuke Nakauchi, Noriaki Kawaguchi, and Takayuki Yanagida

Nara Institute of Science and Technology (NAIST), 8916-5, Takayama-cho, Ikoma-shi, Nara 630-0192, Japan

(Received October 30, 2023; accepted January 9, 2024)

**Keywords:** transparent ceramics, SrF<sub>2</sub>, Eu, scintillator

Eu-doped SrF<sub>2</sub> transparent ceramics were synthesized by spark plasma sintering, and their optical and scintillation properties were studied. The Eu-doped SrF<sub>2</sub> transparent ceramics showed an emission peak at 410 nm with excitations of 250 and 350 nm, and the PL quantum yield of the 0.1% Eu-doped SrF<sub>2</sub> transparent ceramic was 8.1%. Moreover, the Eu-doped SrF<sub>2</sub> transparent ceramics showed scintillation with emission peaks at 300 and 410 nm under X-ray irradiation. Based on the measured scintillation decay times, the origins of the emissions at 300 and 410 nm were self-trapped excitation and 5d–4f transitions of Eu<sup>2+</sup> ions, respectively. The scintillation light yield of the 0.1% Eu-doped SrF<sub>2</sub> transparent ceramic was evaluated to be about 6100 photons/MeV under <sup>137</sup>Cs  $\gamma$ -rays.

## 1. Introduction

Scintillators are a class of phosphors that absorb and immediately convert the energy of incident ionizing radiation to thousands of ultraviolet/visible photons. Attention to new scintillator materials is promoted by an increasing number of new applications such as medical (X-ray CT and PET),<sup>(1)</sup> security,<sup>(2)</sup> particularly the presence of hidden special nuclear materials (SNM oil logging),<sup>(3)</sup> environmental monitoring,<sup>(4)</sup> astronomy,<sup>(5)</sup> and particle physics.<sup>(6)</sup> The most common scintillators are bromides and iodides doped with Tl<sup>+</sup>, Eu<sup>2+</sup>, or Ce<sup>3+</sup> ions such as cesium iodide doped with Tl (CsI:Tl), strontium iodide doped with Eu (SrI<sub>2</sub>:Eu), and lanthanum bromide doped with Ce (LaBr<sub>3</sub>:Ce).<sup>(7,8)</sup> These crystals have high light yield (100000 photons/MeV for SrI<sub>2</sub>:Eu), good energy resolution, and short decay time.<sup>(9)</sup> In general, bromides and iodides have high hygroscopicity and deliquescence, which are disadvantages. In addition, it was reported that SrI<sub>2</sub>:Eu showed the temperature-related instability of the light yield.<sup>(10)</sup> On the other hand, alkaline earth fluorides, which have been applied as scintillators,<sup>(11,12)</sup> have low hygroscopicity, low phonon energy, and high radiation resistance. For instance, barium fluoride (BaF<sub>2</sub>) single crystals are known as scintillator materials. It has been reported that the scintillation of BaF<sub>2</sub> crystals is due to Auger-free luminescence and self-trapped excitation (STE).<sup>(13–17)</sup> In particular, BaF<sub>2</sub> has a relatively large effective atomic number, so it has a great advantage for use in  $\gamma$ -ray detections. Calcium fluoride (CaF<sub>2</sub>) single crystals are known to show

---

\*Corresponding author: e-mail: [kato.takumi.ki5@ms.naist.jp](mailto:kato.takumi.ki5@ms.naist.jp)  
<https://doi.org/10.18494/SAM4749>

scintillation due to STE at 270 nm.<sup>(18–20)</sup> Moreover, it has large band gap energy and relatively high light yield (13000 photons/MeV),<sup>(21)</sup> and CaF<sub>2</sub> has been investigated for potential as the scintillator in astrophysics.<sup>(22)</sup>

Nowadays, almost all the scintillators used in practice are bulk single crystals because they have excellent properties such as high transparency, high light yield, and high detection efficiency due to the volume of bulk single crystals.<sup>(23–25)</sup> On the other hand, recent studies have opened up a new possibility of using transparent ceramics as scintillator materials owing to the achievement of improved synthesis technologies developed with the advancement of the laser field.<sup>(26–29)</sup> In comparison with single crystals, ceramics have many advantages such as cost effectiveness, flexible geometric shape, and mechanical strength. Furthermore, they have also been found to show an equivalent or even superior performance as a scintillator compared with the single crystal form.<sup>(26–28)</sup> However, these studies have only dealt with oxide materials; therefore, we have started to investigate the scintillation properties of halogen compound ceramics with transparent or translucent forms. Thus far, our groups have developed and evaluated CaF<sub>2</sub>, BaF<sub>2</sub>, CsCl, and CsBr transparent ceramics for scintillator applications.<sup>(30–33)</sup>

In this paper, to extend our previous investigations, Eu-doped SrF<sub>2</sub> transparent ceramics were developed by spark plasma sintering (SPS), and their photoluminescence (PL) and scintillation properties were characterized. The fabrication method and optical properties of undoped and Yb-doped SrF<sub>2</sub> transparent ceramics have already been reported.<sup>(34,35)</sup> In addition, we have compared the scintillation properties of transparent ceramics and single crystals of undoped SrF<sub>2</sub>;<sup>(36)</sup> however, no report on the scintillation properties of Eu-doped SrF<sub>2</sub> transparent ceramics can be found.

## 2. Materials and Methods

Eu-doped SrF<sub>2</sub> transparent ceramic samples were synthesized by SPS using Sinter Land LabX-100. Reagent-grade EuF<sub>3</sub> and SrF<sub>2</sub> powders were homogeneously mixed using a mortar, and Eu concentrations were 0.01, 0.1, and 1.0 mol% with respect to SrF<sub>2</sub>. The obtained powder was loaded in a graphite die and sealed with two graphite punches from up and down directions. The graphite was covered with a carbon felt sheet to keep it warm and placed in a furnace to sinter. The sintering conditions used were as follows: the temperature was increased from 20 to 890 °C at a rate of 10 °C/min and held for 10 min while applying a pressure of 10 MPa, and then the temperature was increased to 1080 °C at a rate of 10 °C/min and held for 20 min while applying a pressure of 100 MPa in a vacuum. The surfaces of the sintered samples were optically polished with a polishing machine (MetaServ 250, Buehler).

To investigate the optical properties, transmittance spectra were measured using a spectrophotometer (SolidSpec-3700, Shimadzu) in the spectral range from 200 to 800 nm with 0.5 nm intervals. PL and excitation spectra were measured using a spectrofluorometer (FP8600, JASCO). PL quantum yields (*QY*s) were estimated using Quantaurus-QY (C11347, Hamamatsu Photonics). To calculate PL *QY*, the numbers of absorbed photons ( $N_{absob}$ , 340 nm) and emitted photons ( $N_{emit}$ , from 390 to 600 nm) were determined on the basis of PL intensities with and without the sample, and PL *QY* was calculated as  $QY = N_{emit}/N_{absob}$ . PL decay curves monitored

at 410 nm under 340 nm excitation were measured using Quantaaurus- $\tau$  (C11367, Hamamatsu Photonics). Then, PL decay constants were evaluated by the least-square fitting of decay curves using an exponential decay function.

Radiation-induced luminescence properties were characterized as follows. X-ray-induced scintillation spectra from 250 to 700 nm were measured using a setup.<sup>(28)</sup> A monochromator equipped with a CCD-based detector (Shamrock 163 monochromator and DU-420-BU2 CCD, Andor) was used to measure the scintillation spectra. The sample was attached to an optical fiber, which guided the scintillation light to the detector. The X-ray source used here was an X-ray tube (W anode/Be window) equipped with a generator unit (XRB80N100, Spellman). The supplied tube voltage and current were 80 kV and 1.2 mA, respectively. To measure X-ray-induced scintillation decay curves, we used an afterglow characterization system equipped with a pulse X-ray tube. The obtained information can be found elsewhere.<sup>(37)</sup> A pulse height spectroscopy measurement was conducted to estimate scintillation light yields induced by  $\gamma$ -rays. In the measurement, a sample was firmly placed on a window of the photomultiplier tube (PMT; R877-100, Hamamatsu) using an optical grease (6262 A, OKEN) and covered by several layers of Teflon sheet to guide the scintillation photons to the PMT effectively. A pre-amplifier (113, ORTEC) was subsequently used to amplify PMT output signals, and the signals were processed by a shaping amplifier (572, ORTEC) with a 10  $\mu$ s shaping time. The signal output was integrated and registered using a multichannel analyzer (Pocket MCA 8000 A, Amptek), and then a pulse height spectrum was constructed on a personal computer. In this measurement, a sealed radioactive  $^{137}\text{Cs}$   $\gamma$ -ray was used as the radiation source.

### 3. Results and Discussion

Transmittance spectra are shown in Fig. 1. The thicknesses of the 0.01, 0.1, and 1.0% Eu-doped samples were 0.56, 0.55, and 0.56 mm, respectively. All the samples in the inset were visually transparent and indicated a transmittance of around 60% over a wavelength range of

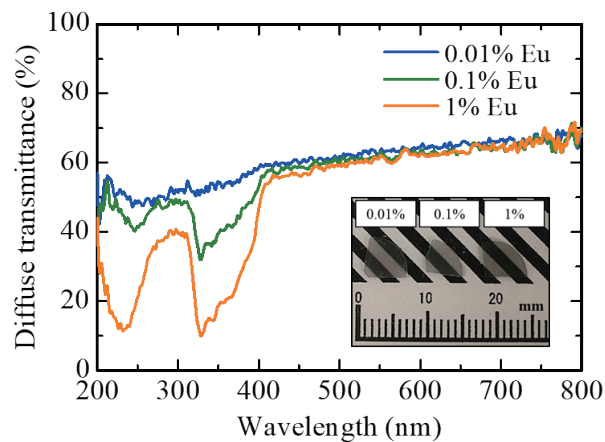


Fig. 1. (Color online) Transmittance spectra from 200 to 800 nm. The inset shows the appearance of the obtained samples.

400–800 nm. Because the band gap of SrF<sub>2</sub> is 11.3 eV (110 nm),<sup>(38,39)</sup> no optical absorption edge was observed in the measurement range. On the other hand, absorption bands were observed at around 230 and 350 nm for all the samples, and the absorptions clearly increased with an increase in dopant concentration. It was considered that these absorptions were due to the 4f–5d transitions of Eu<sup>2+</sup> ions.

PL excitation and emission spectra are presented in Fig. 2. A broad emission band was detected at 410 nm under excitations at 250 and 350 nm. Excitation wavelengths agreed with the absorption wavelengths shown in the transmittance spectra. Similar spectral shapes and positions were reported in earlier works on Eu-doped SrF<sub>2</sub>.<sup>(40)</sup> The *QY* values of the 0.01, 0.1, and 1.0% Eu-doped samples were 5.1, 8.1, and 2.5%, respectively, and the *QY* value of the 0.1% Eu-doped sample was maximum among the present samples. The reason for the low *QY*s is that the samples prepared by SPS often include lattice defects and are contaminated by carbon during sintering. Under 390 nm excitation, PL emission peaks were observed at 590 and 615 nm, originating from the 4f–4f transitions of Eu<sup>3+</sup>.<sup>(41–43)</sup> Figure 3 shows PL decay time profiles when a monitored wavelength was fixed to 410 nm under 340 nm excitation. The decay curves were fitted with an exponential decay function. The delivered decay time constants from the approximation were 380–435 ns, which are consistent with those of Eu<sup>2+</sup> ions.<sup>(44,45)</sup> By these evaluations, we assigned the emission origin of the 410 nm peak to the 5d–4f transitions of Eu<sup>2+</sup> ions.

X-ray-induced scintillation spectra are presented in Fig. 4. Under X-ray irradiation, all the samples showed an emission band at 410 nm due to the 5d–4f transition of Eu<sup>2+</sup> ions as observed in the PL spectra (Fig. 3). In addition to this, all the samples showed an emission band at 300 nm attributed to STE. The scintillation intensity at 300 nm decreased with an increase in Eu concentration. The possible reason is that the local structure of the host lattice was affected by the increase in Eu concentration, so the generation of STE was suppressed.<sup>(46–48)</sup> Moreover, only the 1.0% Eu-doped sample exhibited some remarkable peaks between 450 and 700 nm, which are due to the 4f–4f transitions of Eu<sup>3+</sup> ions.<sup>(41–43)</sup> These characteristics coincided with the spectra of single crystals with the same chemical composition.<sup>(49)</sup>

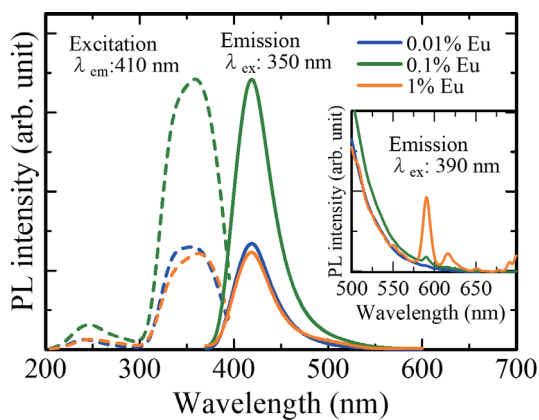


Fig. 2. (Color online) PL excitation and emission spectra. The inset shows emission spectra under 390 nm excitation.

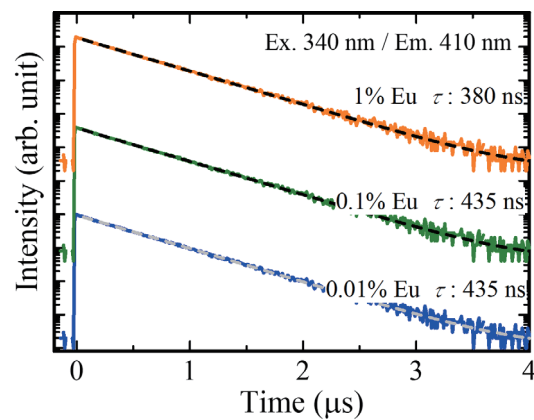


Fig. 3. (Color online) PL decay time profiles under 340 nm excitation.

These assignments were confirmed on the basis of scintillation decay time constants. Figure 5 shows the X-ray-induced scintillation decay time profiles. The scintillation decay curves of all the samples were approximated by a sum of three exponential functions. The obtained decay time constants were 154, 439, and 1107 ns for the 0.1% Eu-doped sample. The first and third decay time constants were consistent with the values due to STE in the previous report.<sup>(50)</sup> The obtained second decay time constants agreed with the PL decay time constants measured in this study and that of 5d–4f transitions of  $\text{Eu}^{2+}$  ions.<sup>(51)</sup>

Figure 6 shows pulse height spectra under  $^{137}\text{Cs}$   $\gamma$ -ray irradiation. The photoabsorption peaks of the 0.01, 0.1, and 1.0% Eu-doped samples appeared at 305, 315, and 110 ch, respectively. The light yield was estimated by comparing the Eu-doped samples with Ce-doped  $(\text{Lu,Y})_2\text{SiO}_5$  (LYSO), showing a light yield of 22000 photons/MeV. The light yields of the 0.01, 0.1, and 1.0% Eu-doped samples were 5900, 6100, and 2100 photons/MeV, respectively. The light yield of the 1.0% Eu-doped sample was smaller than those of the 0.01 and 0.1% Eu-doped samples. This decrease is associated with the decrease in PL  $QY$  calculated under 340 nm excitation and the existence of  $\text{Eu}^{3+}$  ions observed in scintillation spectra. In general, the light yield is proportional

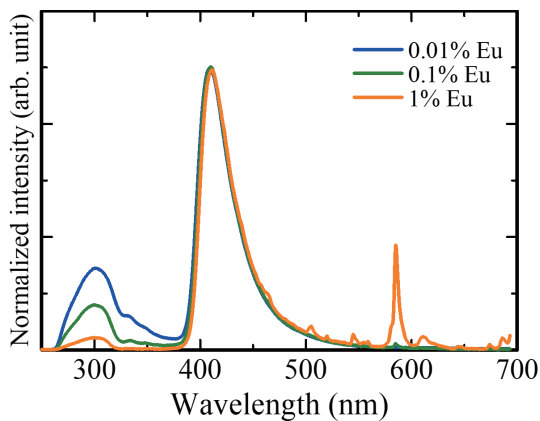


Fig. 4. (Color online) X-ray-induced scintillation spectra.

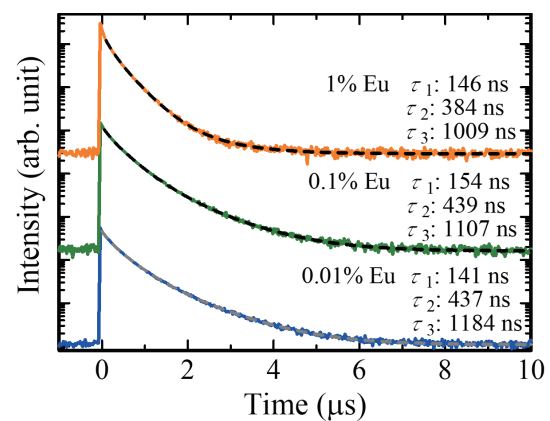


Fig. 5. (Color online) X-ray-induced scintillation decay time profiles.

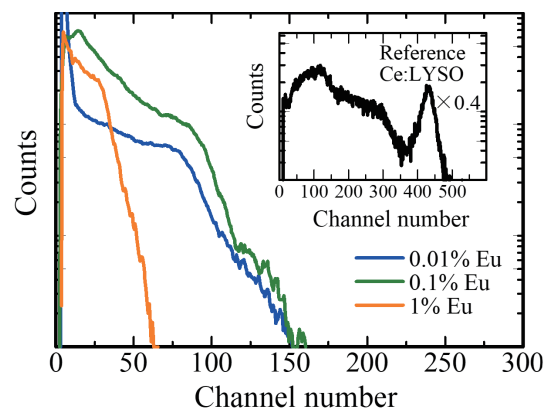


Fig. 6. (Color online) Pulse height spectra under  $^{137}\text{Cs}$   $\gamma$ -ray irradiation.

to PL  $QY$ , and the scintillation from  $\text{Eu}^{3+}$  ions cannot effectively contribute to the light yield owing to its relatively long decay time. Compared with that of Eu-doped  $\text{CaF}_2$  transparent ceramics (17700 photons/MeV), the light yield of Eu-doped  $\text{SrF}_2$  transparent ceramics was low.<sup>(52)</sup>

#### 4. Conclusions

We synthesized Eu-doped  $\text{SrF}_2$  transparent ceramics by SPS and then investigated their optical and scintillation properties. From experimental results of PL and scintillation, it was confirmed that the Eu-doped  $\text{SrF}_2$  transparent ceramics showed the emission peak at 410 nm due to the 5d–4f transitions of  $\text{Eu}^{2+}$  ions. In addition, the 1.0% Eu-doped  $\text{SrF}_2$  exhibited some emission peaks caused by the 4f–4f transitions of  $\text{Eu}^{3+}$  ions. The highest light yield was approximately 6100 photons/MeV among the present samples.

#### Acknowledgments

This work was supported by Grants-in-Aid for Scientific Research A (22H00309), Grants-in-Aid for Scientific Research B (22H03872, 22H02939, 21H03733, and 21H03736), Early-Career Scientists (23K13689), and Challenging Exploratory Research (22K18997) from the Japan Society for the Promotion of Science. The Cooperative Research Project of the Research Center for Biomedical Engineering, Nippon Sheet Glass Foundation, Terumo Life Science Foundation, KRF Foundation, Tokuyama Science Foundation, Iketani Science and Technology Foundation, and Foundation for Nara Institute of Science and Technology are also acknowledged.

#### References

- 1 C. Eijk and W. E. Van: Nucl. Instrum. Methods Phys. Res., Sect. A **509** (2003) 17. [https://doi.org/10.1016/S0168-9002\(03\)01542-0](https://doi.org/10.1016/S0168-9002(03)01542-0)
- 2 J. M. Hall, S. Asztalos, P. Billoft, J. Church, M. A. Descalle, T. Luu, D. Manatt, G. Mauger, E. Norman, D. Petersen, J. Pruet, S. Prussin, and D. Slaughter: Nucl. Instrum. Methods Phys. Res., Sect. B **261** (2007) 337. <https://doi.org/10.1016/j.nimb.2007.04.263>
- 3 T. Yanagida, Y. Fujimoto, S. Kurosawa, K. Kamada, H. Takahashi, Y. Fukazawa, M. Nikl, and V. Chani: Jpn. J. Appl. Phys. **52** (2013) 076401. <https://doi.org/10.7567/JJAP.52.076401>
- 4 K. Watanabe: Jpn. J. Appl. Phys. **62** (2023) 010507. <https://doi.org/10.35848/1347-4065/ac90a5>
- 5 K. Yamaoka, M. Ohno, Y. Terada, S. Hong, J. Kotoku, Y. Okada, A. Tsutsui, Y. Endo, K. Abe, Y. Fukazawa, S. Hirakuri, T. Hiruta, K. Itoh, T. Itoh, T. Kamae, M. Kawaharada, N. Kawano, K. Kawashima, T. Kishishita, T. Kitaguchi, M. Kokubun, G. M. Madejski, K. Makishima, T. Mitani, R. Miyawaki, T. Murakami, M. M. Murashima, K. Nakazawa, H. Niko, and M. Nomachi: IEEE Trans. Nucl. Sci. **52** (2005) 2765. <https://doi.org/10.1109/TNS.2005.862778>
- 6 T. Itoh, T. Yanagida, M. Kokubun, M. Sato, R. Miyawaki, K. Makishima, T. Takashima, T. Tanaka, K. Nakazawa, T. Takahashi, N. Shimura, and H. Ishibashi: Nucl. Instrum. Methods Phys. Res., Sect. A **579** (2007) 239. <https://doi.org/10.1016/j.nima.2007.04.144>
- 7 T. Yanagida, K. Watanabe, T. Kato, D. Nakauchi, and N. Kawaguchi: Sens. Mater. **35** (2023) 423. <https://doi.org/10.18494/SAM4135>
- 8 T. Yanagida, T. Kato, D. Nakauchi, and N. Kawaguchi: Jpn. J. Appl. Phys. **62** (2023) 010508. <https://doi.org/10.35848/1347-4065/ac9026>
- 9 T. Yanagida, M. Koshimizu, G. Okada, and T. Kojima: Opt. Mater. **61** (2016) 119. <https://doi.org/10.1016/j.optmat.2016.05.030>



- 10 M. S. Alekhin, J. T. M. de Haas, K. W. Krämer, I. V. Khodyuk, L. de Vries, and P. Dorenbos: IEEE Nucl. Sci. Symp. Med. Imaging Conf. (2010). <https://doi.org/10.1109/NSSMIC.2010.5874044>
- 11 R. Shendrik, E. A. Radzhabov, and A. I. Nepomnyashchikh: Radiat. Meas. **56** (2013) 58. <https://doi.org/10.1016/j.radmeas.2013.01.054>
- 12 N. Kawaguchi, T. Kato, D. Nakauchi, and T. Yanagida: Jpn. J. Appl. Phys. **62** (2023) 010611. <https://doi.org/10.35848/1347-4065/ac99c3>
- 13 M. R. Farukhi and C. F. Swinehart: IEEE Trans. Nucl. Sci. **18** (1971) 200. <https://doi.org/10.1109/TNS.1971.4325864>
- 14 V. Nanal, B. B. Back, and D. J. Hofman: Nucl. Instrum. Methods Phys. Res., Sect. A **389** (1997) 430. [https://doi.org/10.1016/S0168-9002\(97\)00326-4](https://doi.org/10.1016/S0168-9002(97)00326-4)
- 15 M. Laval, M. Moszyński, R. Allemand, E. Cormoreche, P. Guinet, R. Odru, and J. Vacher: Nucl. Instrum. Methods Phys. Res. **206** (1983) 169. [https://doi.org/10.1016/0167-5087\(83\)91254-1](https://doi.org/10.1016/0167-5087(83)91254-1)
- 16 P. P. Fedorov, S. V. Kuznetsov, A. N. Smirnov, E. A. Garibin, P. E. Gusev, M. A. Krutov, K. A. Chernenko, and V. M. Khanin: Inorg. Mater. **50** (2014) 738. <https://doi.org/10.1134/S002016851407005X>
- 17 C. Hu, L. Zhang, R. Y. Zhu, A. Chen, Z. Wang, L. Ying, and Z. Yu: Nucl. Instrum. Methods Phys. Res., Sect. A **950** (2020) 162767. <https://doi.org/10.1016/j.nima.2019.162767>
- 18 L. P. Cramer, T. D. Cumby, J. A. Leraas, S. C. Langford, and J. T. Dickinson: J. Appl. Phys. **97** (2005) 103533. <https://doi.org/10.1063/1.1904725>
- 19 V. B. Å. Mikhailik, H. Kraus, J. Imber, and D. Wahl: Nucl. Instrum. Methods Phys. Res., Sect. A **566** (2006) 522. <https://doi.org/10.1016/j.nima.2006.06.063>
- 20 W. Chen, L. Ma, R. Schaeffer, R. Hoffmeyer, T. Sham, G. Belev, S. Kasap, and R. Sammynaiken: J. Phys. Conf. Ser. **619** (2015) 012047. <https://doi.org/10.1088/1742-6596/619/1/012047>
- 21 R. A. Heaton and C. C. Lin: Phys. Rev. B **22** (1980) 3629. <https://doi.org/10.1103/PhysRevB.22.3629>
- 22 Y. Shimizu, M. Minowa, W. Suganuma, and Y. Inoue: Phys. Lett. B **633** (2006) 195. <https://doi.org/10.1016/j.physletb.2005.12.025>
- 23 H. Fukushima, D. Nakauchi, T. Kato, N. Kawaguchi, and T. Yanagida: Sens. Mater. **35** (2023) 429. <https://doi.org/10.18494/SAM4139>
- 24 K. Okazaki, D. Nakauchi, H. Fukushima, T. Kato, N. Kawaguchi, and T. Yanagida: Sens. Mater. **35** (2023) 459. <https://doi.org/10.18494/SAM4144>
- 25 P. Kantuptim, D. Nakauchi, T. Kato, N. Kawaguchi, and T. Yanagida: Sens. Mater. **34** (2022) 603. <https://doi.org/10.18494/SAM3690>
- 26 T. Yanagida, H. Takahashi, T. Ito, D. Kasama, T. Enoto, M. Sato, S. Hirakuri, M. Kokubun, K. Makishima, T. Yanagitani, H. Yagi, T. Shigeta, and T. Ito: IEEE Trans. Nucl. Sci. **52** (2005) 1836. <https://doi.org/10.1109/TNS.2005.856757>
- 27 T. Yanagida, Y. Fujimoto, Y. Yokota, K. Kamada, and S. Yanagida: Radiat. Meas. **46** (2011) 1503. <https://doi.org/10.1016/j.radmeas.2011.03.039>
- 28 T. Yanagida, K. Kamada, Y. Fujimoto, H. Yagi, and T. Yanagitani: Opt. Mater. **35** (2013) 2480. <https://doi.org/10.1016/j.optmat.2013.07.002>
- 29 J. Lu, M. Prabhu, J. Song, C. Li, J. Xu, K. Ueda, A. A. Kaminskii, H. Yagi, and T. Yanagitani: Appl. Phys. B **71** (2000) 469. <https://doi.org/10.1007/s003400000394>
- 30 F. Nakamura, T. Kato, G. Okada, N. Kawaguchi, and K. Fukuda: J. Eur. Ceram. Soc. **37** (2017) 1707. <https://doi.org/10.1016/j.jeurceramsoc.2016.11.016>
- 31 T. Kato, G. Okada, K. Fukuda, and T. Yanagida: Radiat. Meas. **106** (2017) 140. <https://doi.org/10.1016/j.radmeas.2017.03.032>
- 32 H. Kimura, F. Nakamura, T. Kato, D. Nakauchi, N. Kawano, G. Okada, N. Kawaguchi, and T. Yanagida: Optik **157** (2018) 421. <https://doi.org/10.1016/j.ijleo.2017.11.104>
- 33 H. Kimura, F. Nakamura, T. Kato, D. Nakauchi, G. Okada, N. Kawaguchi, and T. Yanagida: Sens. Mater. **30** (2018) 1555. <https://doi.org/10.18494/sam.2018.1923>
- 34 W. Li, B. Mei, J. Song, and Z. Wang: Mater. Lett. **159** (2015) 210. <https://doi.org/10.1016/j.matlet.2015.06.105>
- 35 W. Li, H. Huang, B. Mei, and J. Song: Opt. Mater. **75** (2018) 7. <https://doi.org/10.1016/j.optmat.2017.10.009>
- 36 T. Kato, N. Kawano, G. Okada, N. Kawaguchi, K. Fukuda, and T. Yanagida: Optik **168** (2018) 956. <https://doi.org/10.1016/j.ijleo.2018.04.082>
- 37 T. Yanagida, Y. Fujimoto, T. Ito, K. Uchiyama, and K. Mori: Appl. Phys. Express. **7** (2014) 5. <https://doi.org/10.7567/APEX.7.062401>
- 38 T. Demkiv, M. Chylii, V. Vistovskyy, A. Zhyshkovich, N. Gloskovska, P. Rodnyi, A. Vasil'ev, A. Gektin, and A. Voloshinovskii: J. Lumin. **190** (2017) 10. <https://doi.org/10.1016/j.jlumin.2017.05.036>

- 39 R. Jia, H. Shi, and G. Borstel: *Comput. Mater. Sci.* **43** (2008) 980. <https://doi.org/10.1016/j.commatsci.2008.02.012>
- 40 M. Y. A. Yagoub, H. C. Swart, R. E. Kroon, and E. Coetsee: *Phys. B* **535** (2018) 310. <https://doi.org/10.1016/j.physb.2017.08.011>
- 41 S. Asada, G. Okada, T. Kato, F. Nakamura, N. Kawano, N. Kawaguchi, and T. Yanagida: *Chem. Lett.* **47** (2018) 59. <https://doi.org/10.1246/cl.170940>
- 42 N. Kawano, T. Kato, G. Okada, N. Kawaguchi, and T. Yanagida: *Opt. Mater.* **88** (2019) 67. <https://doi.org/10.1016/j.optmat.2018.11.002>
- 43 S. Matsumoto, T. Watanabe, and A. Ito: *Sens. Mater.* **34** (2022) 669. <https://doi.org/10.18494/SAM3698>
- 44 Y. Onoda, H. Kimura, T. Kato, K. Fukuda, N. Kawaguchi, and T. Yanagida: *Optik* **181** (2019) 50. <https://doi.org/10.1016/j.jjleo.2018.11.160>
- 45 M. Y. A. Yagoub, H. C. Swart, L. L. Noto, P. Bergman, and E. Coetsee: *Materials* **8** (2015) 2361. <https://doi.org/10.3390/ma8052361>
- 46 Y. Lan, B. Mei, W. Li, F. Xiong, and J. Song: *J. Lumin.* **208** (2019) 183. <https://doi.org/10.1016/j.jlumin.2018.12.047>
- 47 A. I. Nepomnyashchikh, E. A. Radzhabov, A. V. Egranov, and V. F. Ivashchkin: *Radiat. Meas.* **33** (2001) 759. [https://doi.org/10.1016/S1350-4487\(01\)00101-9](https://doi.org/10.1016/S1350-4487(01)00101-9)
- 48 E. Radzhabov: *J. Phys. Condens.* **486** (2002) 458. [https://doi.org/10.1016/S0168-9002\(02\)00753-2](https://doi.org/10.1016/S0168-9002(02)00753-2)
- 49 K. Kawano, T. Ohya, T. Tsurumi, K. Katoh, and R. Nakata: *Phys. Rev. B: Condens. Matter* **60** (1999) 11984. <https://doi.org/10.1103/PhysRevB.60.11984>
- 50 R. Lindner, R.T. Williams, and M. Reichling: *Phys. Rev. B: Condens. Matter* **63** (2001) 1. <https://doi.org/10.1103/physrevb.63.075110>
- 51 H. Kimura, T. Kato, D. Nakauchi, N. Kawaguchi, and T. Yanagida: *Sens. Mater.* **34** (2021) 691. <https://doi.org/10.18494/SAM3687>
- 52 F. Nakamura, T. Kato, G. Okada, N. Kawaguchi, K. Fukuda, and T. Yanagida: *Ceram. Int.* **43** (2017) 604. <https://doi.org/10.1016/j.ceramint.2016.09.201>